Available online at www.sciencedirect.com

ScienceDirect

Procedia CIRP 123 (2024) 440–445

www.elsevier.com/locate/procedia

7th CIRP Conference on Surface Integrity

Chip Morphology Prediction in Inconel 718 Milling through Machine Learning to Control Surface Integrity

Omkar Mypati[a], Hakan Dogan[b], Jose A. Robles-Linares[a], Alborz Shokrani[b], Zhirong Liao[a,*]

[a]*Machining and Condition Monitoring Group, Faculty of Engineering, University of Nottingham, Nottingham, NG8 1BB, United Kingdom*

[b]*Department of Mechanical Engineering, University of Bath, Bath, BA2 7AY, United Kingdom*

* Corresponding author. Tel.: +44-775-427-785. E-mail address: Zhirong.Liao@nottingham.ac.uk

Abstract

A nickel-based aerospace superalloy, Inconel 718 presents machining challenges because of its hardness and strength. Monitoring and predicting chip morphology during milling is essential for early defect detection and process optimisation. This study examines the correlation between sensor signals with surface roughness and chip morphology in milling Inconel 718 using machine learning (ML). Due to progressive tool wear and heat generation, the surface roughness varies in addition to the chip exhibiting different morphologies, such as continuous, discontinuous, and oxidised chips. AE signals were analysed in the time and frequency domains to identify chip morphology transitions. An accelerometer captured cutting vibration signals that showed higher instability during discontinuous chip formation. Chip colour due to oxidization varies with milling forces as a result of tool wear. Based on multiple sensor data fusion, a random forest model predicts better chip morphology from different machining parameters. The integrated ML system enables real-time monitoring of chip morphology mechanisms through diverse signals. This permits early diagnosis of surface integrity and chip morphologies indicating imminent tool wear. The approach enhances process stability and tool life when milling difficult-to-machine alloys. It demonstrates the viability of relating sensor signals to fundamental mechanisms through AI for intelligent machining.

Keywords: Nickel-based alloy; Chip morphology; Machine learning; Senors; Real-time monitoring

1. Introduction

Inconel 718 is a precipitation-hardened nickel-chromium alloy used extensively in aerospace components like gas turbine engines due to its high-temperature strength, corrosion resistance, and oxidation resistance [1,2]. Its unique properties, however, make machining this alloy a complex process. These include remarkable strength, hardness, toughness, low thermal conductivity, and a tendency to adhere to cutting tools. However, Inconel 718 contains abrasive carbide inclusions, resulting in work-hardening and consequent tool wear [3]. This, in parallel with rising temperatures at the tool-chip interface, which are enabled due to the alloy's low thermal conductivity, leads to complex changes in chip morphology [4], which can vary from discontinuous to segmented or even serrated patterns [6,8] and distinct colouration are observed [5]. Generally, the continuous chips are formed at relatively low cutting speeds; they appear as long ribbon-like curled segments, indicating stable plastic deformation through shear plane localization, where the surface roughness is relatively low. Discontinuous saw-tooth-shaped chips are produced at intermediate cutting speeds due to adiabatic shear band propagation, leading to unstable segmented chip formation, where the surface roughness of the sample exhibits higher [5,6].

The chip colouration appears at high cutting speeds or when severe plastic deformation is present (i.e., enabled by tool wear) [7] as a result of thermochemical oxidation at elevated temperatures. This induces the formation of thin, stable oxide layers on the segmented chips, giving rise to varying shades of coloured chip formation [8]. The transitions between the

10.1016/j.procir.2024.05.077

surface roughness and chip morphologies provide vital macroscale evidence of the changing microscale material separation mechanisms, cutting forces, and thermomechanical conditions at the tool-workpiece interface [9]. For instance, the saw-tooth discontinuous chips indicate deterioration of tool condition and loss of process stability. Therefore, real-time monitoring of chip morphology enables us to maintain good surface integrity of the workpiece and early diagnosis of undesirable transitions well before catastrophic tool failure. The in-process chip morphology monitoring offers a pivotal route to enhance productivity and reliability when machining difficult-to-cut materials e.g., Inconel 718, Ti6Al4V/SiC fibre MMCs [10–12].

Very few research has focused on leveraging multi-sensor signals to quantify chip characteristics objectively. Sensors, including dynamometers, accelerometers, acoustic emission sensors, and motor current sensors, can capture force, vibration, and acoustic signatures sensitive to chip morphology shifts [13]. During the machining of Inconel 718, the sensor signals in the time domain contain distinct signatures correlating to chip morphology changes [5,6]. Cutting forces exhibit lower steady levels for continuous chips but higher fluctuating amplitudes for discontinuous segmented chips due to the pulsed nature of shear band formation [14]. Vibration signals also demonstrate more intense spikes coinciding with each serrated chip segment being formed, indicating a loss of cutting stability [5].

Similarly, acoustic emission sensors detect increased modulation and ringing corresponding to the repetitive fracture events, producing discontinuous chips [6]. The consistently generated coloured chips from oxidation are due to the elevated temperature resulting from high cutting force levels throughout the machining cycle [15]. This elevated temperature is based on enhanced tool-chip contact friction from wear [5]. Advanced signal processing and machine learning (ML) techniques enable automated chip classification by extracting these morphology-sensitive features from multi-sensor data. The fusion of advanced sensor analytics and artificial intelligence algorithms enables automated, real-time classification of chip morphology in machining processes [16]. ML techniques are leveraged to establish correlations between the raw sensor streams and microscopic chip characteristics [17,18]. This study uses an instrumented machining setup with integrated sensors to monitor the milling of Inconel 718 superalloy. The objective is to relate the sensor signals to surface roughness, chip morphology and tool wear progression, enabling early detection of undesirable tool conditions to minimise damage to the machined surface integrity.

2. Experimental setup and data acquisition

Inconel 718 machining experiments were conducted on a 3-axis Haas vertical milling machine. A 5-flute with 5µm TiSiN-coated EMT100 end mill (Harmetal), with 12 mm diameter, 0.5 mm Corner radius, 10.5° Radial rake angle, 13.5° Axial rake angle and 48° helix angle, was utilised for each experiment. The cutting parameters (Table 1) were held constant for all tests. Inconel 718 samples (150x50x50 mm^3) were rigidly clamped to the milling machine's worktable to minimise vibration during machining. The workpiece was oriented such that the feed direction was parallel to the length of the part (i.e., total cutting length of 150 mm). This setup enabled tool wear and chip morphology monitoring over an extended cutting length for each experiment. No coolant was employed to intentionally promote progressive tool wear.

Table 1. Tool geometry and cutting parameters.

Parameters	Cutting speed (m/min)	Feed (mm/ tooth)	Axial depth of cut (mm)	Radial depth of cut (mm)
Values	30	0.05	1	5

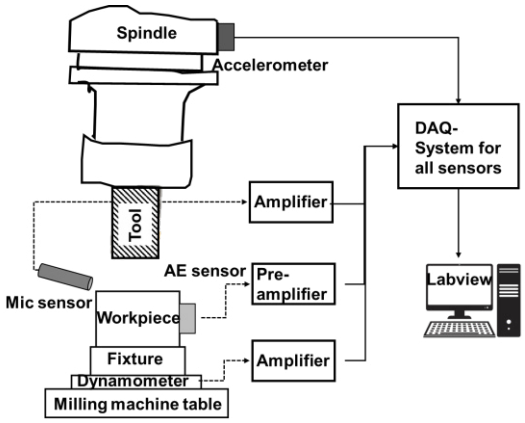

Fig 1. Schematic representation of machine tool with position of various sensors for process monitoring

The milling process was instrumented with various sensors for in-situ monitoring, as shown in Fig 1. The Kistler dynamometer used for cutting force measurement has a sampling rate of 1 kHz. The Dytran triaxial accelerometer acquires vibration data at 10 kHz. This high rate enables tracking acceleration peaks at failure-prone spindle speeds and aids in the early detection of tool damage. Acoustic emission signals contain high-frequency components sampled at 1 MHz using a Kistler sensor and a NI 9775 data acquisition system. This level of detail is indispensable to relate signals to the underlying physics of chip formation and tool wear mechanisms when machining difficult-to-cut alloys like Inconel 718. The collected sensor data was then pre-processed to train and test ML models for chip morphology classification. As illustrated in Fig. 2, the approach involves acquiring force, vibration, acoustic emission, and microphone signals during milling. These multi-sensor signals are segmented into windows and subjected to feature extraction in the time, frequency, and time-frequency domains. Principle component analysis ranks the most relevant features for chip morphology prediction. The features are input into ML models to determine the optimal classifier. The models first identify present chip morphology from sensor features. The same models then predict morphological evolution by analysing features extracted from forecasted future signal values. The developed model enables data-driven monitoring and prediction of chip formation for intelligent machining.

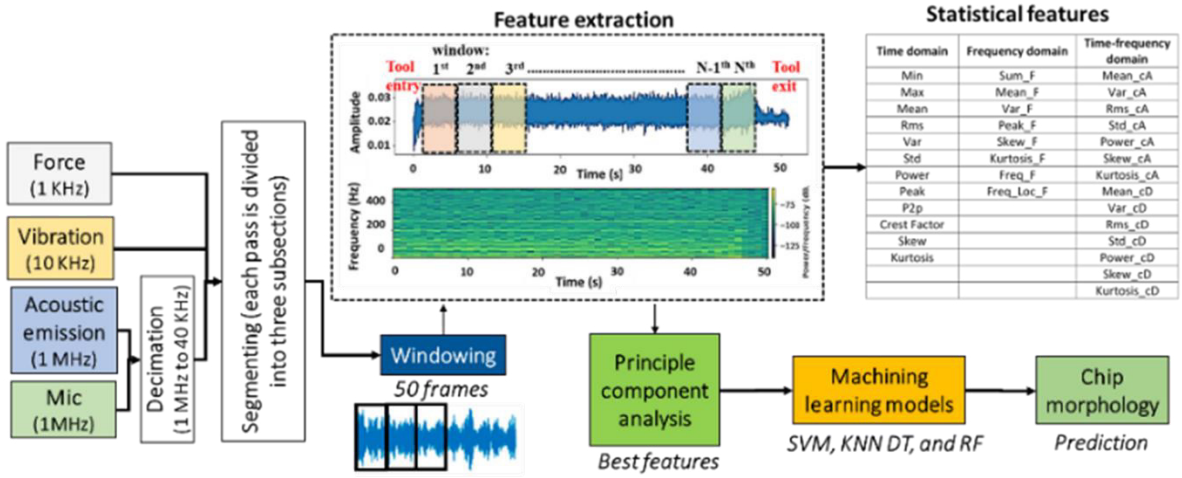

F - Frequency feature, cA - approximate component feature, cD – detail component feature

Fig 2. The proposed method for monitoring and predicting the chip morphology

3. Results and discussion

3.1 Tool wear and chip morphology correlation

The progression of tool wear during the end milling of Inconel 718 workpieces was monitored by measuring flank wear using an optical microscope camera after each milling pass. A total of 5 passes were conducted with a constant cutting speed of 30 m/min, feed per tooth of 0.05 mm, and radial depth of cut of 5 mm. The flank wear on the peripheral cutting edges was quantified after each cut by capturing microscope images for analysis, as shown in Fig 3. This revealed a gradual growth in wear land width as the number of cutting passes increased. Specifically, the wear measurements were 0.08 mm, 0.11 mm, 0.17 mm, 0.25 mm, and 0.32 mm (notch wear) after the 1st, 2nd, 3rd, 4th, and 5th passes, respectively. The diffuse wear land became increasingly noticeable on the tool's clearance face with longer machining duration. This wear progression is attributed primarily to abrasion from the hard oxide particles in the Inconel 718 work material, coupled with plastic deformation and adhesion due to the high temperatures and pressures [19]. The trend highlights the importance of wear monitoring and tool replacement criteria when machining nickel superalloys, which accelerate tool degradation.

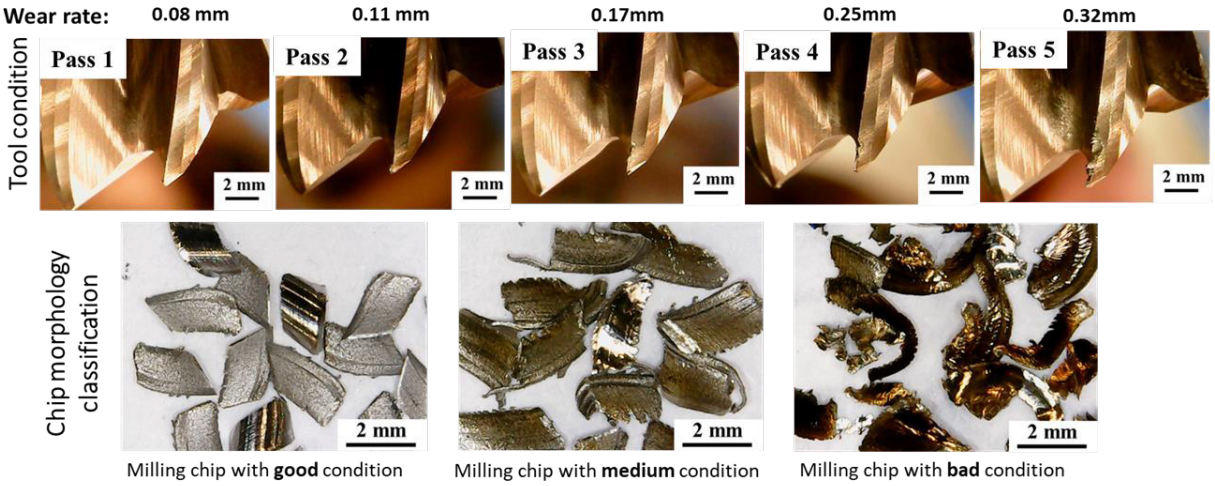

Fig 3. Tool wear measurement after each cutting pass and classified chip morphology based on tool wear progression

In rising flank wear, the morphology of the formed chips was also observed to change significantly. In the initial passes with sharp tools, discontinuous uniform-shaped chips with uniform colouring were produced, as shown in Fig 3. However, as the wear land widened, the chips became increasingly segmented with non-uniform colouring. Light red-coloured segments began appearing along the chips, indicating temperature variations during formation. The segmentation is likely caused by deterioration of the tool's cutting edge, leading to cyclic sticking and release of the chips. This alters the strain, temperature, and friction experienced by the chip formation. The diverse chip morphologies and colours provide visual cues that correlate to the quantification of tool flank wear. Therefore, monitoring chip characteristics provides an indirect, relatively straightforward to identify excessive cutting tool wear during nickel alloy machining. The observations underscore the close linkage between evolving tool conditions and alterations in chip formation mechanics during milling. To further investigate the relationship between tool wear and chip morphology, sensor signals were acquired during each milling

pass to capture the dynamics of the cutting process. The sensor data streams were segmented and subjected to feature extraction to generate relevant inputs for developing an ML model. The model was trained to classify chip morphology into three categories - good, acceptable, and bad - based on the quantified flank wear measurements from the microscope analysis. 'Good' morphology corresponded to uniform coloured continuous chips produced in the sharp tool state with wear less than 0.15 mm. 'acceptable' denoted partially segmented chips with some colour variations, correlating to the transition wear range of 0.15-0.25 mm. Finally, 'bad' morphology refers to thoroughly segmented chips with highly coloured segments associated with wear exceeding 0.25 mm.

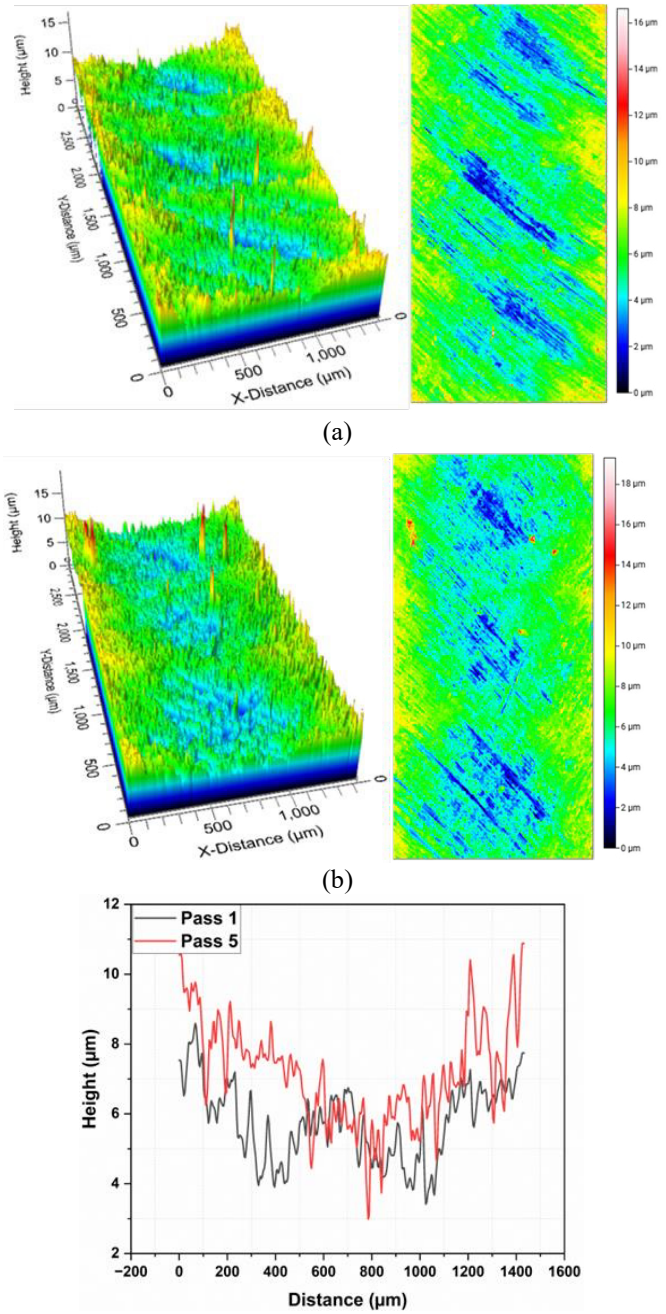

Fig 4. Surface roughness for the samples at (a) pass 1, (b) pass 5, and (c) variation of surface peak

3.2 Tool wear and surface roughness correlation

As tool wear progresses during machining, the cutting-edge profile of the tool deteriorates, leading to an increase in the surface roughness of the machined workpiece. The gradual abrasion wear, adhesion, and diffusion effects blunt the sharp cutting edges, causing them to rub against the workpiece rather than shear cleanly. This plowing action produces rough peaks and valleys on the previously smooth-cut surface. Additionally, the built-up edge and uneven wear land lead to inconsistent contact conditions between the tool and workpiece, generating surface variations as shown in Fig 4 a, b and c. The changes in chip formation and morphology noted previously provide visual evidence of this dynamic. As flank wear exceeded 0.25 mm, significant segmentation and colour variation in the chips indicated a cyclic sticking and release pattern induced by the worn tool's engagement. This non-uniform cutting phenomenon directly translates to surface roughness escalation. Surface profilometry measurements quantitatively confirmed that average roughness (R_a) increased monotonically from 0.27 µm in the initial cut to 0.48 µm after the final 5th pass. The metrics showed a strong correlation to the quantified tool flank wear growth per pass, affirming the interdependency between tool wear progression and surface finish degradation. This emphasises the critical need for wear monitoring and tool change strategies to not only protect part quality but also ensure dimensional accuracy. The collected dataset establishes a baseline for the development of predictive models linking tool conditions to achieve workpiece surface integrity.

3.3 Best Statistical Feature Selection

Adequate condition monitoring through sensor analytics relies on extracting informative features that capture relevant signatures from the raw data. For a complex process like machining, the multi-sensor measurements, including vibrations, acoustics and forces, contain valuable information about the machining process. Statistical techniques like time-domain moments, frequency-domain transforms, and time-frequency distributions can be applied to derive over 37 statistical features. However, not all these features provide unique value for building predictive models. Using redundant, irrelevant features can degrade the model's performance and interpretability. In this work, a principal component analysis (PCA) is used in the identification of the most important statistical features through dimensionality reduction. PCA transforms the high-dimensional feature space into fewer principal component dimensions that explain the maximum variance [20]. This is achieved by computing the eigenvectors of the feature covariance matrix. The eigenvectors define an uncorrelated subspace ordered by the amount of variation captured from the original feature set. By retaining only, the top 10 principal components, PCA reduced the 37 statistical features down to 10 dominant features that preserved the most helpful information. The ten features identified through PCA maximised the captured variance while minimising redundancy. For the acoustic emission, vibration, and force

signals, the number of features reduced by PCA are depicted in Fig 5a, b, and c, respectively.

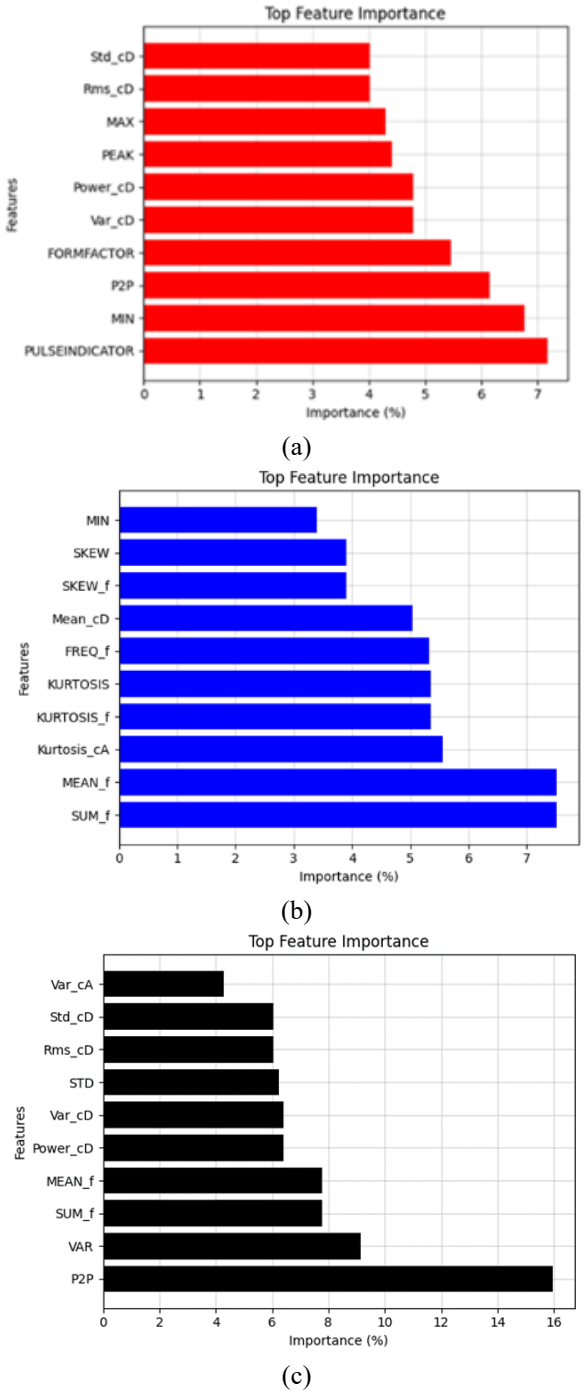

Fig 5. Feature selection using PCA analysis for (a) acoustic emission signal, (b) vibration, and (c) force sensor signals

3.4 Chip morphology detection

A range of ML models were applied to identify the optimal approach for predicting chip morphology based on key statistical features of the chip production process. The data was split into training (75%), testing (15%) and validation (15%) sets. Four standard ML algorithms were tested: Decision Tree (DT), Random Forests (RF), K-Nearest Neighbour (KNN), and Support Vector Machines (SVM). The models were trained on the training set and optimised using the validation set before final testing on the unseen test set, and the results are listed in Table 2.

Table 2: Accuracy metrics of the various ML models for chip morphology prediction

	ML model	Accuracy
1	Decision tree (DT)	98.64
2	Random forest (RF)	99.81
3	K-nearest Neighbors (KNN)	88.45
4	Support vector machines (SVM)	92.57

The RF model achieved the best performance with a test accuracy of 99.81%. This ensemble method creates multiple decision trees on bootstrapped sub-samples of the training data, averaging the predictions to reduce variance and avoid overfitting. The bagging process builds trees using a random subset of features, further de-correlating the trees to improve generalisation. Gini impurity was used as the splitting criterion to measure the homogeneity of node samples. Pre-pruning was applied to prevent overfitting. The DT model achieved 98.64% accuracy using a single CART tree grown on the whole training set, selecting optimal splits via information gain. While less prone to overfitting, performance is limited by high variance which the RF ensemble addresses by averaging predictions across de-correlated trees. SVM achieves 92.57% accuracy, which attempts to find the maximum margin hyperplane dividing classes using a radial basis function kernel. Grid search found optimal parameters for the validation set, but this higher bias model underfits. KNN makes predictions by identifying the k most similar training samples and majority voting, but performance dropped significantly to 88.45% due to the curse of dimensionality

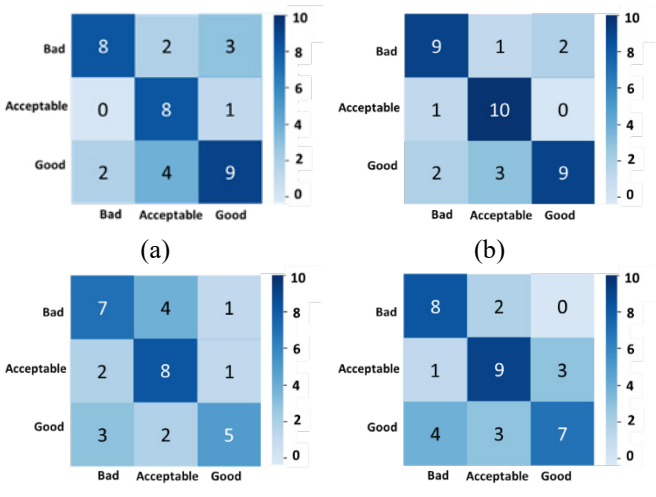

Fig 6. Confusion matrix analysis of various ML models (a) DT, (b) RF, (c) KNN, and (d) SVM

The RF model shows the true positive rate is exceptionally high at 99%, indicating nearly all chip classes are correctly classified, as shown in Fig 6b. The true negative rate is also high, rarely misclassifying as a negative case. The overall true positive and true negative rates demonstrate the RF model reliably identifies the chip morphology. The DT confusion matrix tells a similar story, with true positive and negative rates of 98% and 97%, respectively, as shown in Fig 6a. However, the increased errors highlight the limitations of relying on a

single tree. KNN shows much lower true positive and negative rates of only 80% and 92%, respectively, reflecting its poorer performance, as shown in Fig 6c. The SVM confusion matrix indicates a relatively high false positive rate of 8%, meaning it is more likely to classify a negative case compared to RF and DT incorrectly, as depicted in Fig 6d. Hence, the RF model shows the best accuracy at nearly 100% on unseen test data. RF avoids overfitting by combining diverse decision trees and maintains high true positive and negative rates. This interpretable ensemble approach is an optimal solution for predicting chip morphology, given its performance on key statistical features of the manufacturing process.

4. Conclusion

Prolonged machining of difficult-to-machine materials such as Inconel 718 can induce rapid tool wear with a cutting tool. Tool wear is often manifested as detrimental changes in chip morphology, such as increased segmentation and coloured chips. Based on the present study, chip morphology transitioned from uniform-coloured continuous chips at 0.08 mm wear to thoroughly segmented and discoloured chips above 0.25 mm wear. This demonstrates chip characteristics can indicate tool wear state. Further, the correlation between progressive tool wear and surface roughness confirms that tool monitoring is necessary for maintaining machined part surface integrity over prolonged machining of nickel superalloys. Based on the predictions, the RF model performed superior to other algorithms, achieving 99.81% accuracy on unseen test data. In addition, the RF model achieved an excellent 99% true positive rate and 99.5% true negative rate, reliably identifying chip morphology. In addition, there is potential to further extend the study to predict the subsurface plastic deformation layer depth utilising multi sensor-based machine learning models.

Acknowledgements

The authors acknowledge the support of the United Kingdom Engineering and Physical Sciences Research Council (EPSRC) through grant number EP/V055011/1 for project SENSYCUT.

References

[1] A. De Bartolomeis, S.T. Newman, I.S. Jawahir, D. Biermann, A. Shokrani, Future research directions in the machining of Inconel 718, J Mater Process Technol. 297 (2021). https://doi.org/10.1016/j.jmatprotec.2021.117260.

[2] D. Xu, L. Ding, Y. Liu, J. Zhou, Z. Liao, Investigation of the influence of tool rake angles on machining of inconel 718, Journal of Manufacturing and Materials Processing. 5 (2021). https://doi.org/10.3390/jmmp5030100.

[3] A. de Bartolomeis, S.T. Newman, D. Biermann, A. Shokrani, State-of-the-art cooling and lubrication for machining inconel 718, Journal of Manufacturing Science and Engineering, Transactions of the ASME. 143 (2021). https://doi.org/10.1115/1.4047842.

[4] G. Zhang, S. To, G. Xiao, The relation between chip morphology and tool wear in ultra-precision raster milling, Int J Mach Tools Manuf. 80–81 (2014) 11–17. https://doi.org/10.1016/j.ijmachtools.2014.02.005.

[5] C. Liu, M. Wan, W. Zhang, Y. Yang, Chip Formation Mechanism of Inconel 718: A Review of Models and Approaches, Chinese Journal of Mechanical Engineering (English Edition). 34 (2021). https://doi.org/10.1186/s10033-021-00552-9.

[6] B. Wang, Z. Liu, Acoustic emission signal analysis during chip formation process in high speed machining of 7050-T7451 aluminum alloy and Inconel 718 superalloy, J Manuf Process. 27 (2017) 114–125. https://doi.org/10.1016/j.jmapro.2017.04.003.

[7] S.-H. Chen, Z.-R. Luo, Study of using cutting chip color to the tool wear prediction, The International Journal of Advanced Manufacturing Technology. 109 (2020) 823–839. https://doi.org/10.1007/s00170-020-05354-2.

[8] A. Gregorio, T. Santos, R. Rossi, A. Jesus, J. Outeiro, P. Rosa, A. Tribology, P. Stief, J.-Y. Dantan, A. Etienne, A. Siadat, Tribology of metal cutting: newly: newly formed underside of chip, Procedia CIRP. 82 (2019) 136–141. https://doi.org/10.1016/j.procir.2019.04.034.

[9] D. Axinte, H. Huang, J. Yan, Z. Liao, What micro-mechanical testing can reveal about machining processes, Int J Mach Tools Manuf. 183 (2022). https://doi.org/10.1016/j.ijmachtools.2022.103964.

[10] G. Ortiz-de-Zarate, A. Sela, M. Saez-de-Buruaga, M. Cuesta, A. Madariaga, A. Garay, P.J. Arrazola, Methodology to establish a hybrid model for prediction of cutting forces and chip thickness in orthogonal cutting condition close to broaching, International Journal of Advanced Manufacturing Technology. 101 (2019) 1357–1374. https://doi.org/10.1007/s00170-018-2962-1.

[11] S. Zan, Z. Liao, J.A. Robles-Linares, G. Garcia Luna, D. Axinte, Machining of long ceramic fibre reinforced metal matrix composites – How could temperature influence the cutting mechanisms?, Int J Mach Tools Manuf. 185 (2023). https://doi.org/10.1016/j.ijmachtools.2023.103994.

[12] L. Li, H. Chen, Z. Liao, Y. Yang, D. Axinte, Investigation of the grain deformation to orthogonal cutting process of the textured Alloy 718 fabricated by laser powder bed fusion, Int J Mach Tools Manuf. 190 (2023). https://doi.org/10.1016/j.ijmachtools.2023.104050.

[13] K.T. Chung, A. Geddam, A multi-sensor approach to the monitoring of end milling operations, J Mater Process Technol. 139 (2003) 15–20. https://doi.org/10.1016/S0924-0136(03)00175-4.

[14] M.C. Kang, J.S. Kim, J.H. Kim, A monitoring technique using a multi-sensor in high speed machining, J Mater Process Technol. 113 (2001) 331–336. https://doi.org/https://doi.org/10.1016/S0924-0136(01)00698-7.

[15] D. Hajdu, A. Astarloa, I. Kovacs, Z. Dombovari, The curved uncut chip thickness model: A general geometric model for mechanistic cutting force predictions, Int J Mach Tools Manuf. 188 (2023). https://doi.org/10.1016/j.ijmachtools.2023.104019.

[16] E. Emel, E. Kannatey-Asibu, Acoustic emission and force sensor fusion for monitoring the cutting process, Int J Mech Sci. 31 (1989) 795–809. https://doi.org/10.1016/0020-7403(89)90025-8.

[17] S. Omole, H. Dogan, A.J.G. Lunt, S. Kirk, A. Shokrani, Using machine learning for cutting tool condition monitoring and prediction during machining of tungsten, Int J Comput Integr Manuf. 00 (2023) 1–25. https://doi.org/10.1080/0951192X.2023.2257648.

[18] O. Mypati, A. Mukherjee, D. Mishra, S.K. Pal, P.P. Chakrabarti, A. Pal, A critical review on applications of artificial intelligence in manufacturing, Springer Netherlands, 2023. https://doi.org/10.1007/s10462-023-10535-y.

[19] X. Li, X. Liu, C. Yue, S.Y. Liang, L. Wang, Systematic review on tool breakage monitoring techniques in machining operations, Int J Mach Tools Manuf. 176 (2022). https://doi.org/10.1016/j.ijmachtools.2022.103882.

[20] I.T. Jollife, J. Cadima, Principal component analysis: A review and recent developments, Philosophical Transactions of the Royal Society A: Mathematical, Physical and Engineering Sciences. 374 (2016). https://doi.org/10.1098/rsta.2015.0202.